CONSTRUCTIVE-FUNCTIONAL AND FEM ANALYSIS OF AN OIL UOP 12 C1 PUMP

CAMELIA-GEORGIANA ADAMACHE[1], GEORGIANA-ALEXANDRA MOROSANU[2*], NICUSOR BAROIU[2,3]

[1] Bayards Helideck Bv, Nieuw-Lekkerland, zip Code 2957 CP, Netherlands; cameliaadamache@gmail.com
[2] Research Center in Manufacturing Engineering Technology (ITCM), "Dunărea de Jos" University of Galati, 111 Domnească Street, 800201, Galati, Romania; Alexandra.Costin@ugal.ro
[3] "Dunărea de Jos" University of Galati, Faculty of Engineering, 111 Domnească Street, Galati, 800201, Romania; Nicusor.Baroiu@ugal.ro
* Correspondence: Alexandra.Costin@ugal.ro;

Received: 08.10.2025
Revised: 27.10.2025
Accepted: 04.11.2025
Published: 08.12.2025

Abstract: The paper presents the constructive-functional and FEM analysis of an oil UOP 12 C1 pump, aiming at three-dimensional modeling of the assembly in Autodesk Inventor program, as well as the finite element analysis of the created graphical model, determining the minimum and maximum values for the state of stresses and displacements. The stages of creating the 3D model, the commands used in the modeling process, as well as the simulation conditions applied in the FEM analysis are detailed. The paper also includes a comparative analysis of the states of stresses and displacements of the pump, depending on the material used - aluminum or steel.

Keywords: oil pump, Autodesk Inventor, FEM analysis

1. INTRODUCTION

Vehicle maintenance is often a challenge for most drivers, with the high cost of services provided by specialized personnel being one of the main discouraging factors. However, keeping the vehicle in optimal operating parameters is as important as saving money. Changing the oil is an important operation, recommended at an interval of 10 000-15 000 kM or once a year, depending on the manufacturer's instructions [1-3].

Although many interventions should be carried out in authorized workshops, certain maintenance tasks, such as changing the oil, can be carried out by the owner. This operation also involves replacing the oil filter, an essential component for retaining impurities that can compromise the durability and performance of the engine. Engine oil is a complex mixture made up of base oils, obtained by distillation of petroleum or synthesis of hydrocarbons, and a package of specialized additives [3].

These components give the oil essential properties for the optimal operation of internal combustion engines, such as reducing friction and wear, cleaning deposits, protecting against corrosion and dissipating heat generated during operation [4-6].

* Corresponding author, email: alexandra.costin@ugal.ro
https://doi.org/10.29081/jesr.v31i1.001

Lubrication is an essential process in the operation of internal combustion engines, ensuring the reduction of friction between moving components and preventing their premature wear. By forming a thin pellicle of oil between metal surfaces, direct contact is limited, energy losses through friction are minimized and it contributes to the dissipation of heat generated during operation.

In the absence of effective lubrication, engine performance can be severely affected and the risk of failure increases considerably, which emphasizes the vital role of the components responsible for oil distribution in the powertrain assembly [4, 5].

Given the importance of correct engine lubrication, the systems responsible for oil circulation become essential components in the structure of a vehicle. Among them, the oil pump plays an important role in ensuring a constant and adequate flow of lubricant to the areas subject to friction and wear [7-10].

Despite the wide use of oil pumps in automotive and industrial systems, detailed constructive-functional and finite element (FEM) analyses for small-scale pumps such as the UOP 12 C1 model are limited in the literature. The lack of comprehensive studies integrating CAD modeling with FEM simulations restricts the understanding of material behavior and performance optimization in real operating conditions. Therefore, it is essential to evaluate the structural and functional characteristics of this type of pump to ensure reliability, safety, and efficiency.

This paper aims to present a complete constructive-functional and FEM analysis of the UOP 12 C1 oil pump. The study includes: the 3D modeling of the pump assembly using Autodesk Inventor, the FEM analysis of the pump base and rotor and a comparative assessment of the mechanical behavior for two materials - steel and aluminum, under identical loading conditions. The results provide useful insights for optimizing material selection and improving the design of oil pumps in similar applications.

2. EXPERIMENTAL SETUP

2.1. Constructive-functional analysis of an oil UOP 12 C1 pump

The UOP 12 C1 type oil pump belongs to the category of hydraulic vane pumps. They are built in constant flow and variable flow versions. The constant flow vane pump (Figure 1) consists of a rotor *2* in which an even number of vanes *1* are mounted, inclined to the rotor radius at an angle α, and a stator *3*.

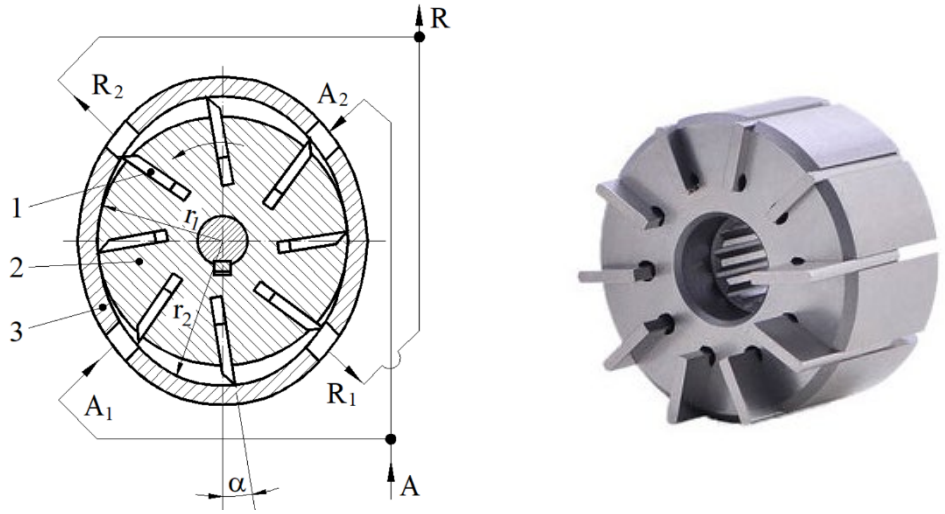

Fig. 1. Constant flow vane pump: A_1, A_2, R_1, R_2 - suction and discharge chambers [11, 12].

The inner profile of the stator is oval, consisting of four circle arcs with radii r_1 and r_2, connected to each other by four portions of an Archimedean spiral. During the rotational movement of the rotor, each pair of vanes delimits, together with the walls of the rotor and the stator, a working chamber that transports the fluid from the suction area, *A*, to the discharge area, *R* [11, 12].

The vane pump with variable flow has the same operating principle as the vane pump with constant flow, with the difference that the rotor axis is offset from the stator axis by a certain eccentricity. In these types of pumps, the fluid transport chamber is formed by vanes, contained in a rotor, whose rotation axis is offset from the stator axis of symmetry by a certain eccentricity. Due to the unilateral loading, the maximum working pressure of some variable flow vane pumps can reach up to 100÷180 bar [11].

The flow rate of the constant flow vane pump is calculated with the relationship:

$$Q = 10^{-6} \cdot V \cdot n \left[\frac{L}{\min}\right] \quad (1)$$

where V is the unit volume (specific flow rate) and is calculated with the relationship:

$$V = 2 \cdot b \cdot \left[\pi(r_2^2 - r_1^2) - \frac{a \cdot z}{\cos \alpha}(r_2 - r_1)\right] \ [\text{mm}^3] \quad (2)$$

where r_1 and r_2 represents the small radius, respectively the large radius of the stator, in mm; b - width of the blades, in mm; a - thickness of the blades, in mm; z - number of blades; α – angle of inclination of the blades.

The approximate calculation relationship for the flow rate at speed n will be:

$$Q = 2 \cdot 10^{-6} \cdot b \cdot n \cdot \left[\pi(r_2^2 - r_1^2) - \frac{a \cdot z}{\cos \alpha}(r_2 - r_1)\right] \ \left[\frac{L}{\min}\right] \quad (3)$$

Due to the fact that the flow rate also depends on the difference in the squares of the radii $r_2^2 - r_1^2$, a pump built for a certain flow rate can be transformed to give a lower flow rate by increasing the radius r_1 or a higher one by increasing the radius r_2.

The driving torque of the vane pump, to achieve a certain pressure, can be calculated with a relationship of the form of relationship (4), in which the unit volume V is determined with relationship (2).

$$M = \frac{p \cdot V}{2 \cdot \pi} \cdot 10^{-4} \ [N \cdot m] \quad (4)$$

where: p is the working pressure, in bars; V - the pump volume, in mm^3.

The technical data of the UOP 12 C1 oil pump are presented in Table 1 [13].

Table 1. Technical data of the UOP 12 C1 pump [13].

No.	Model number	UOP 12 C1
1	Input voltage [V]	12
2	Power [W]	60
3	Maximum operating time, t_{max} [min.]	30
4	Maximum temperature, θ_{max} [°C]	60
5	Protection class	III
6	Clasificarea IP	IPX4
7	Output (pump capacity)* [L/min]:	-
	- diesel / heating oil	aprox. 1.5
	- engine oil (60°C)	aprox. 0.2
8	Discharge capacity [m]	max. 0.7
9	Maximum acceptable pressure [bar]	3
10	Weight (including accessories) [g]	aprox. 890
11	Approximate sound pressure level [dB(A)]	70
*The capacity may differ from the given data, depending on temperature and oil type.		

Figure 2 shows the UOP 12 C1 oil pump. The functional analysis of this type of pump focuses on how it performs its primary function of extracting oil from a tank or system and transferring it to a storage container. These types of pumps are used in various automotive and industrial applications where a constant flow of oil under pressure is

required. It is recommended that oil pumps are not used to discharge flammable liquids such as gasoline, petroleum or other oils. The discharge of water, chemicals, lyes, food, paints or varnishes is also not allowed [13].

The UOP 12 C1 pump is not designed for continuous operation. It can be operated continuously for a maximum of 30 minutes. Any other use not mentioned in the instructions in the user manual may cause damage to the device or may pose a serious risk of injury to the operator [13].

Fig. 2. UOP 12 C1 oil pump [13]: 1 - on / off switch; 2 - pump housing; 3 - battery connection cable; 4 - negative terminal (-) (black); 5 - positive terminal (+) (red); 6 - suction hose, diameter 6 mm; 7 - connector for the discharge hose (*OUT*); 8 - hose clamp; 9 - connector for the suction hose (*IN*); 10 - protective caps; 11 - discharge hose, diameter 12 mm.

2.2. Graphical modeling of the UOP 12 C1 oil pump

Graphical modeling is an important step in the analysis, design and optimization of components. Through CAD technologies, it is possible to obtain a virtual product from the early stages of development, providing a clear and detailed image of the geometry of the parts, the assembly method, as well as the interactions between the components. This approach allows the identification of possible design errors before the creation of physical prototypes, significantly reducing the time and costs associated with the manufacturing process. Also, 3D modeling facilitates direct integration with numerical simulation software, being an indispensable step for performing structural, thermal or dynamic analyses on assemblies [14-18].

The dimensions of the UOP 12 C1 pump were determined by measuring all components using an electronic caliper, Profi Scale Precise PS 7215 (Figure 3 and Figure 4).

Each component of the oil pump was modeled in Autodesk Inventor, the **.ipt* module, the 3D assembly being obtained in the **.iam* module [18]. The components were created using the commands available in the **.ipt* module, such as *Line*, *Circle*, *Extrude*, *Revolve*, *Hole* etc. each being used according to the specific geometry of the part to reproduce the real shape and dimensions of the elements as precisely as possible.

These modeling tools allow generating of the two-dimensional sketches, their transformation into 3D models and the addition of the necessary functional details, thus ensuring a complete and accurate representation of each element in the pump assembly.

Fig. 3. Pump at the time of removing the housing and the cap.

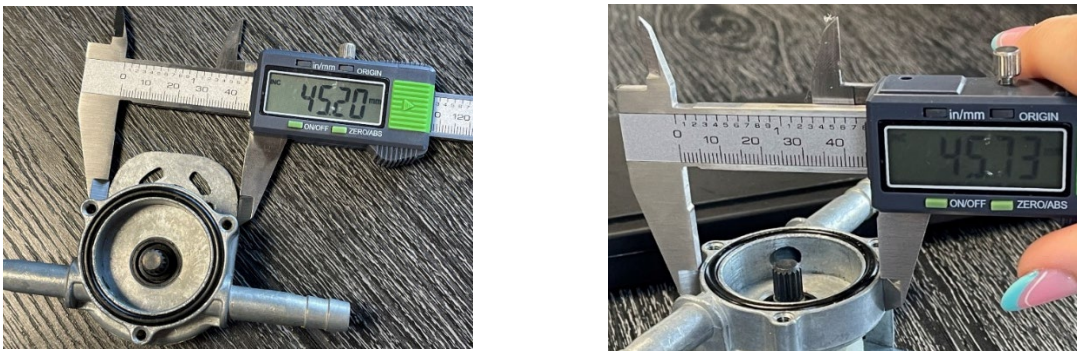

Fig. 4. Oil pump measurement.

Also, in the assembly module, **.iam*, constraints were used that help in joining all the components in an assembly, such as *Mate*, *Offset Constraint*, *Flush*, *Grounded*, *Rotation* etc. [18]. Thus, in Figures 5÷9, some of the 3D components are presented, as well as the assembly of the UOP 12 C1 oil pump, made in the *Autodesk Inventor* program.

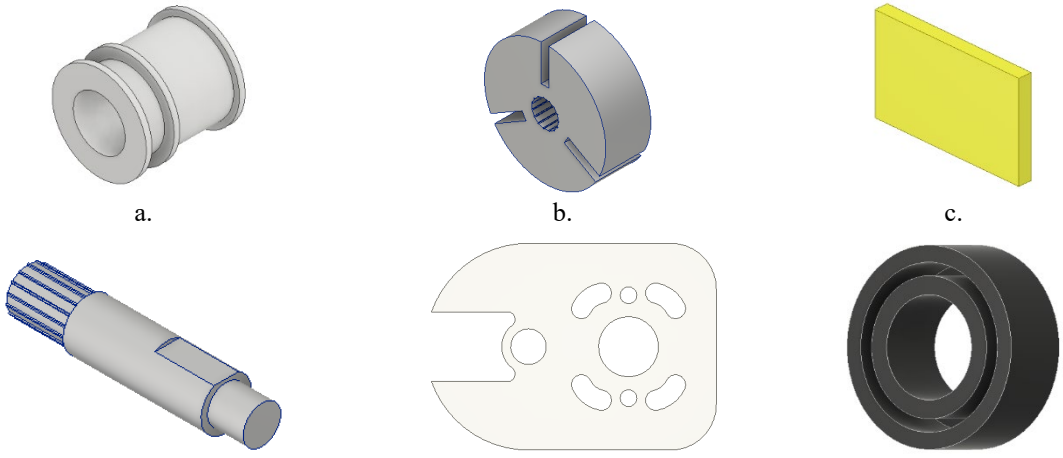

a. b. c.

d. e. f.

Fig. 5. Graphical representation of some components within the oil pump: a - safety seal; b - rotor; c - rotor vane; d - pinion; e - pump base; f - lower seal.

Fig. 6. The assembly between the base and gears.

Fig. 7. The assembly between the base and rotor.

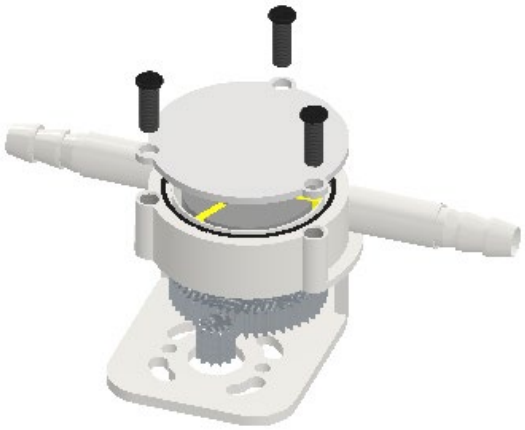

Fig. 8. The assembly between the base, cap and screws.

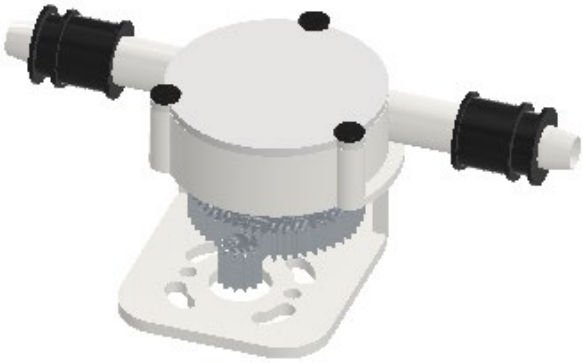

Fig. 9. Virtual model of the UOP 12 C1 oil pump.

2.3. Finite element analysis of the "pump base and rotor" assembly

Finite element analysis (*FEM*) is a fundamental method in evaluating the structural behavior of components subjected to different types of stresses. The application of this method allows the estimation of the stress distribution, displacements and the identification of critical areas in terms of mechanical strength, without the need for physical testing of prototypes. The paper presents the structural analysis of the assembly formed by the pump base and its rotor, using the *FEM* analysis module available in *Autodesk Inventor* program. The aim is to compare the mechanical behavior of the assembly depending on two different materials - aluminum and steel - under the same loading and fixing conditions.

This analysis allows highlighting the advantages and limitations of each material, contributing to the substantiation of decisions related to the optimal choice of materials for such applications [19-22]. Therefore, Table 2 presents the mechanical properties of the two materials.

Table 2. Mechanical properties of the chosen materials.

No.	Proprieties	Steel	Aluminum 6061
1	Mass density [g/cm^3]	7.85	2.7
2	Yield strength [MPa]	207	275
3	Ultimate tensile strength [MPa]	345	310
4	Young's modulus [GPa]	210	68.9
5	Poisson's ratio [ul]	0.3	0.33
6	Shear modulus [GPa]	80.7692	25.9023

To ensure the reproducibility and clarity of the numerical setup, the finite element model was configured with explicitly defined boundary and loading conditions. The pressure load applied to the suction–discharge chamber and to the rotor surfaces was set to 3 bar (0.3 MPa), corresponding to the maximum operating pressure specified in Table 1. The gravitational acceleration was applied globally, acting along the vertical axis, with a value of 9.81 m/s². The fixed constraint was assigned to the lower mounting surface of the pump base, simulating its real fastening to the pump housing during operation.

The contact interaction between the rotor and the pump base was defined as bonded, representing a non-sliding interface consistent with the tight assembly tolerances of the analyzed components. The finite element discretization was automatically generated using 10-node tetrahedral elements, with an average element size of approximately 1.2 mm, corresponding to 0.1 of the model diameter, and a grading factor of 1.5 to ensure mesh refinement in curved and high-stress areas.

The static structural analysis was performed assuming a linear-elastic behavior for both materials (steel and aluminum). The convergence criterion for displacements was set to 1×10^{-4} mm, with a maximum of 50 iterations per load step. Material nonlinearities were neglected, as the applied stresses remained well below the yield limits of the analyzed materials. These conditions ensure the repeatability of the analysis and the validity of the comparative results obtained for the two material configurations.

The analyzed assembly is subjected to external loading and fixing conditions. The *Fixed Constraint* is applied to the pump base. The pressure and gravitational acceleration loads are distributed both on the base and on the rotor, using the specific functions in the program, *Pressure* and *Gravity* (Figures 10÷13).

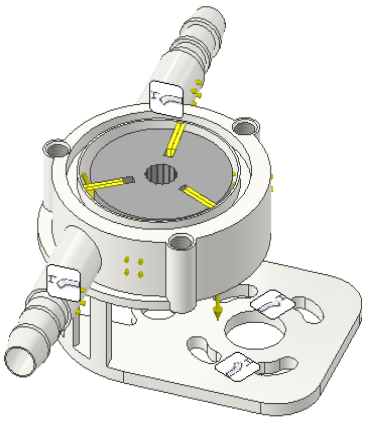

Fig. 10. Applying a fixed support to the pump base.

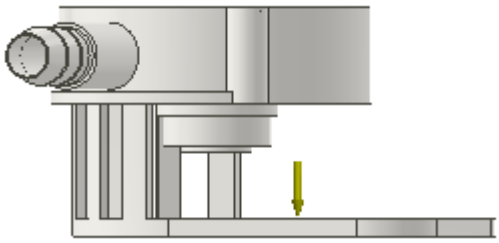

Fig. 11. Applying gravitational acceleration.

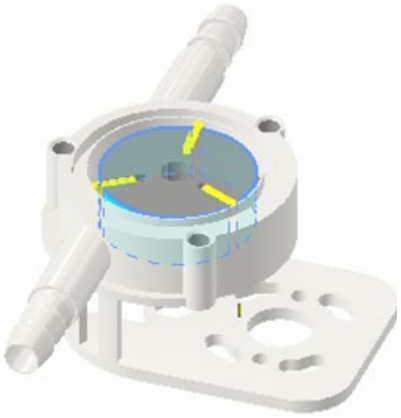

Fig. 12. Applying pressure to suction-discharge chamber.

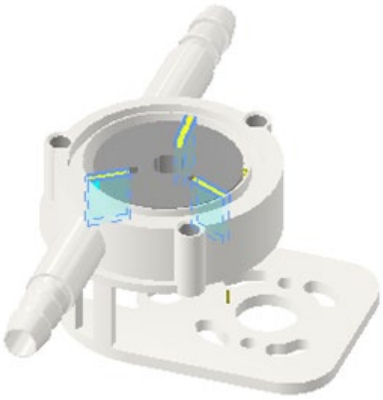

Fig. 13 Applying pressure to the rotor.

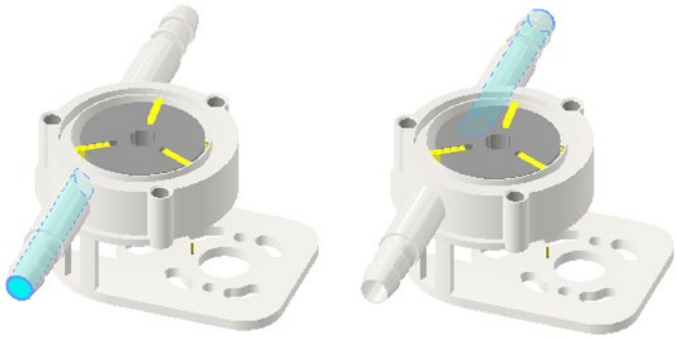

Fig. 14. Applying pressure to the suction-discharge pipes.

In order to generate the discretization, the automatic generation mode with tetrahedral elements was used, the solid assembly being discretized into 45742 elements and 77533 nodes, Figure 15 and Table 3.

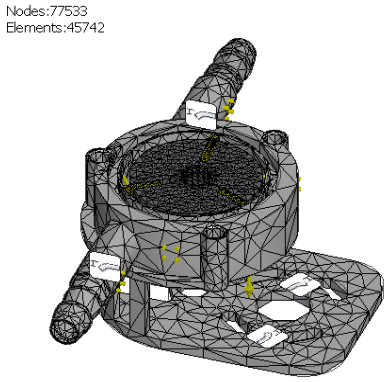

Fig. 15. Finite element discretization.

Table 3. Discretization settings.

No.	Proprieties	Values
1	Average element size (fraction of model diameter)	0.1
2	Minimum element size (fraction of average size)	0.2
3	Grading factor	1.5
4	Maximum turn angle [°]	60
5	Create curved mesh elements	No
6	Shear modulus [GPa]	0.1

3. RESULTS AND DISCUSSION

The displacements result for the case where the pump is made of steel are graphically represented in Figures 16÷19 and centralized in Table 4.

Table 4. Results regarding elastic displacements of the pump base and rotor assembly - steel material.

No.	Name	Minimum	Maximum
1	Volume [mm^3]	34104.7	
2	Mass [kg]	0.266913	
3	Von Mises Stress [MPa]	0.0000152207	10.0863
4	1st Principal Stress [MPa]	-2.96962	9.73738
5	3rd Principal Stress [MPa]	-9.07883	4.91326
6	Displacement [mm]	0	0.000915579
7	Safety Factor [ul]	15	15

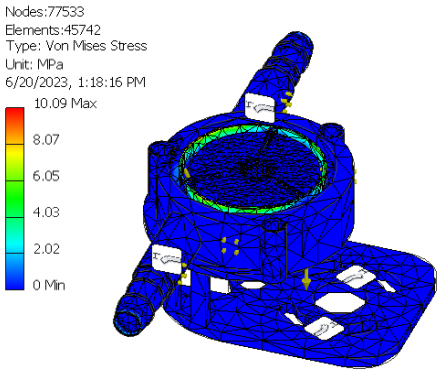

Fig. 16. Equivalent stresses - steel material.

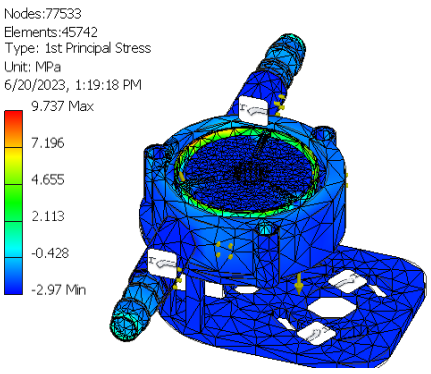

Fig. 17. Normal stress - steel material.

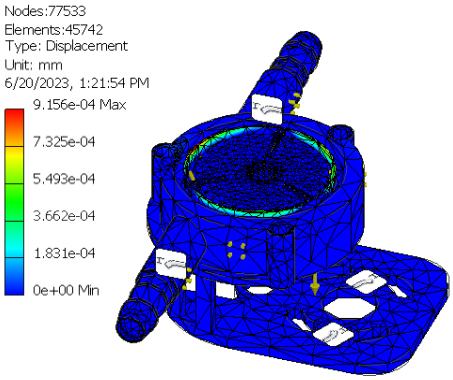

Fig. 18. Displacement - steel material.

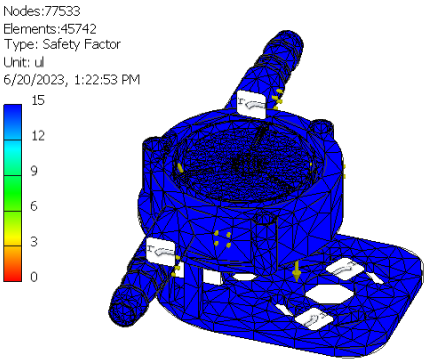

Fig. 19. Safety factor - steel material.

For the situation where the pump base and rotor assembly is made of aluminum, the same constraints and loads are maintained, the discretization having the same number of elements and nodes as in the previous case. The deformation results are expressed in Figures 20÷23 and centralized in Table 5.

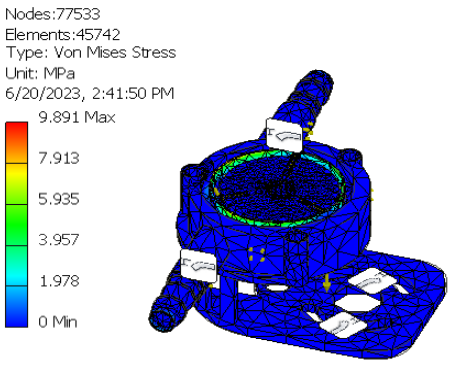

Fig. 20. Equivalent stresses - aluminum material.

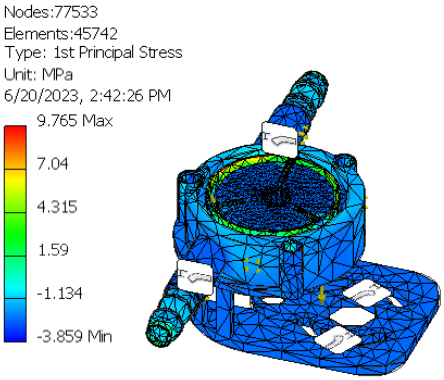

Fig. 21. Normal stress - aluminum material.

Following the FEM analysis carried out on the ”pump base and rotor” assembly, it is observed that, in terms of equivalent stresses (Von Mises), the steel material presents a higher value, of 10.09 MPa, compared to 9.891 MPa in the case of aluminum (Figure 24). This difference, although not major, indicates a higher structural rigidity of the steel under the given conditions. In terms of normal stresses, aluminum registers a slightly higher value (9.765 MPa) compared to steel (9.737 MPa), which suggests a more uniform distribution of stresses, but also a potential increased sensitivity to directed stresses.

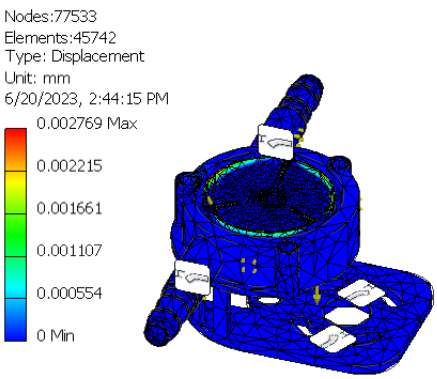

Fig. 22. Displacement - aluminum material.

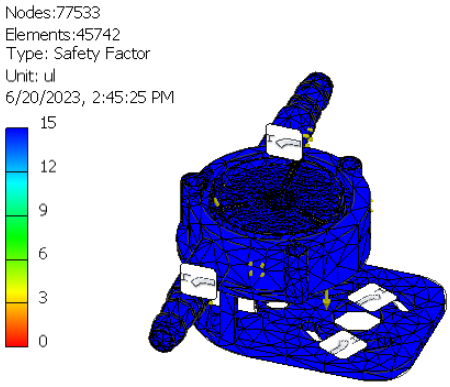

Fig. 23. Safety factor - aluminum material.

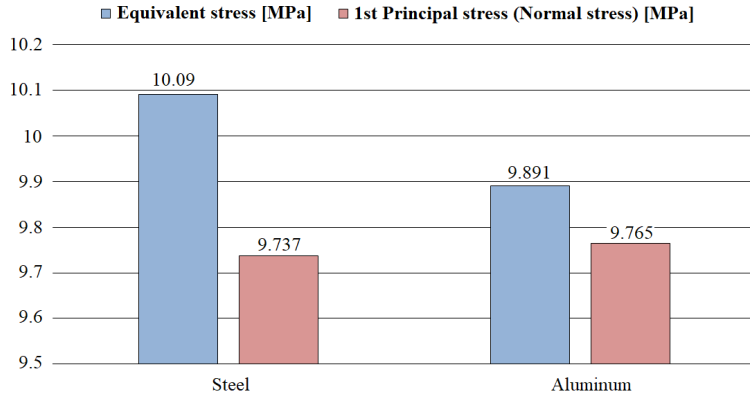

Fig. 24. Graphical representation of equivalent and normal stresses.

In terms of maximum displacements (Figure 25), aluminum, with a deformation of $27.6 \cdot 10^{-4}$ mm, exhibits a deformability approximately three times greater than steel, which exhibits a displacement of only $9.15 \cdot 10^{-4}$ mm.

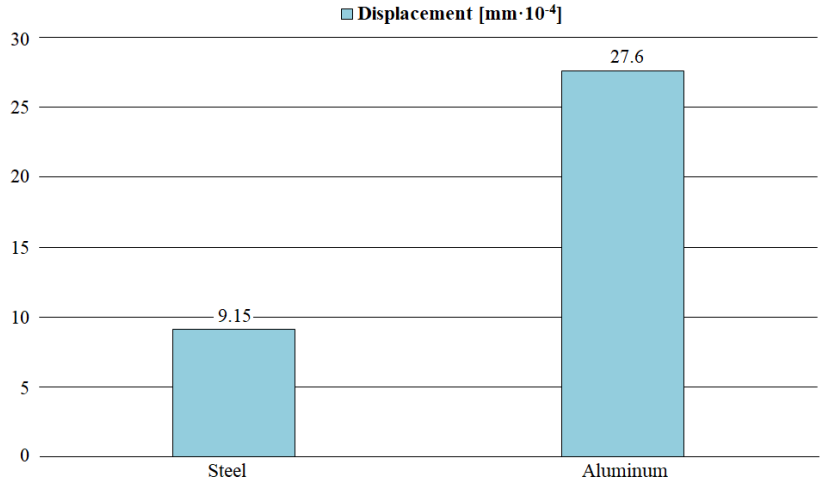

Fig. 25. Graphical representation of the displacement.

This behavior is mainly determined by the lower elastic modulus of aluminum, which leads to greater flexibility of parts made of this material. Thus, although aluminum can contribute to reducing the mass of the assembly and to a faster response in applications, it also involves higher risks of deformation, especially under high load conditions or in environments with frequent vibrations.

4. CONCLUSIONS

In the context of a continuous evolution of the automotive industry, as well as the need to ensure the reliability of mechanical systems, oil pumps have an important role in maintaining the performance and durability of engines. The correct choice of materials and optimization of component design directly contribute to increasing efficiency and reducing maintenance costs.

The study demonstrated that the choice of material significantly influences both the structural rigidity and the deformation characteristics of the pump components:

- for the steel configuration, the *Von Mises equivalent stress* reached a maximum of 10.09 MPa, with a *maximum displacement* of only 0.00092 mm;
- in comparison, the aluminum version showed a *Von Mises stress* of 9.89 MPa and a *maximum displacement* approximately three times higher (0.00277 mm), due to its lower Young's modulus (68.9 GPa vs. 210 GPa for steel);
- the safety factor remained constant at a value of 15 for both materials, indicating that both designs operate well within acceptable stress limits under the applied loads.

These results confirm that steel provides superior rigidity and reduced deformation, making it more suitable for applications requiring dimensional stability and long-term durability. However, aluminum offers a significant mass reduction (0.0997 kg vs. 0.2669 kg) and could be preferred in systems where weight optimization is critical and the load conditions are moderate.

From a design and manufacturing standpoint, the integration of 3D-CAD modeling and FEM simulation proved essential for accurately evaluating the structural response and identifying critical stress areas before prototyping. In this regard, the CAD modeling of the UOP 12 C1 oil pump, as well as the *FEM* analysis, provided a precise geometrical representation, essential for numerical simulations and for evaluating the behavior of the parts under real operating conditions.

***Funding**: "This research received no external funding"*

***Data Availability Statement:**"The JESR Research Data Policie"*

***Conflicts of Interest**:"The authors declare no conflicts of interest"*

REFERENCES

[1] Terziev, A., Zlateva, P., Ivanov, M., Methodology for energy savings assessment, at engine oil change of road vehicles, E3S Web of Conferences, vol. 404, 2023, pp. 1-9.
[2] Tobar, M.G., Pesantez, K.P., Romero, P.J., Urgiles, R.W., The impact of oil viscosity and fuel quality on internal combustion engine performance and emissions: an experimental approach, Lubricants, vol. 13, no. 4, 2025, pp. 1-20.
[3] Baroiu, N., Moroșanu, G.A., Constructive-functional analysis and sizing hydraulic filters, The Annals of "Dunărea de Jos" University of Galaţi, Fascicle V, Technologies in Machine Building, vol. 39, 2021, pp. 6-11.
[4] Jinlin, Y., Xiaozhou, H., Kinematics analysis and oil film lubrication characteristics in the piston-cylinder interface of a bent-axis-type piston motor, Energies, vol. 17, no. 23, 2024, pp. 1-20.
[5] Duan, L., Li, J., Duan, H., Nanomaterials for lubricating oil application: A review. Friction, vol. 11, 2023, pp. 647-684.
[6] Xia, D., Wang, Y., Liu, H., Yan, J., Lin, H., Han, S., Research progress of antioxidant additives for lubricating oils, Lubricants, vol. 12, no. 4, 2024, pp. 1-27.
[7] Jovanovic, V., Janošević, D., Pavlovic, J., Petrović, N., Lazarević, Đ., Analysis of volumetric regulation of hydraulic pumps in hydrostatic systems, Facta Universitatis Series: Automatic Control and Robotics, vol. 23, no 2, 2024, pp. 145 - 155.
[8] Shi, J., Ziyang, L., Jingcheng, G., Dongjing, C., Xiaotao, L., Ying, L., Jin, Z., Xiangdong, K., Thermal-hydraulic modeling of oil-immersed motor pump, Applied Sciences, vol. 13, no. 16, 2023, pp. 1-18.

[9] Yangfeng, C., Dazhou, L., Peng, Z., Hao, Z., Shengdun, Z., A novel lubricating method of oil pump with self-adaptive adjustment function for transmission, Scientific reports, vol. 15, no. 1, 2025, pp. 1-20.
[10] Baroiu, N., Moroșanu, G.A., Graphical modelling and studies on hydraulic pump parameters, Journal of Industrial Design and Engineering Graphics - JIDEG, vol. 15, no. 2, 2020, pp. 7-12.
[11] Baroiu, N., Moroșanu, G.A., Sisteme de acționare hidraulică (Hydraulic actuation systems), Ed. Academica, Galați, 2022.
[12] Baroiu, N., Vișan, D., Ciocan, O.D., Hidrostatică și pneumatică tehnologică - Îndrumar pentru laborator (Technological hydrostatics and pneumatics - laborator guide), Ed. Academica, Galați, 2018.
[13] Manuals, Ultimate Speed UOP 12 C1 manual. Available online: https://www.usermanuals.au/ultimate-speed/uop-12-c1/manual (accessed on 29.04.2025).
[14] Baroiu, N., MoroSanu, G.A., Teodor, V.G., Craciun, R.S., Paunoiu, V., Use of reverse engineering techniques for inspecting screws surfaces of a helical hydraulic pump, International Journal of Modern Manufacturing Technologies, vol. XIV, no. 2, 2022, pp. 20-29.
[15] Morosanu, G.A., Baroiu, N., Teodor, V.G., Paunoiu, V., Oancea, N., Review on study methods for reciprocally enwrapping surfaces, Inventions, vol. 7, no. 1, 2022, pp. 1-33.
[16] Teodor, V.G., Paunoiu, V., Susac, F., Baroiu, N., Optimization of the measurement path for the car body parts inspection, Measurement, vol. 146, 2019, pp. 15-23.
[17] Berbinschi, S., Teodor, V.G., Baroiu, N., Oancea, N., The substitutive circles family method - graphical aproach in CATIA design environment, vol. 31, 2013, pp. 53-56.
[18] Morosanu, G.A., Tehnici de modelare grafică 3D-CAD (3D-CAD graphical modeling techniques), Ed. Academica, București, 2025.
[19] Belabend, S., Paunoiu, V., Baroiu, N., Khelif, R., Iacob, I., Static structural analysis analytical and numerical of ball bearings, IOP Conf. Series: Materials Science and Engineering, vol. 968, 2020, pp. 1-9.
[20] Zharkevich, O., Reshetnikova, O., Nikonova, T., Berg, A., Berg, A., Zhunuspekov, D., Nurzhanova, O., CFD-FEM analysis for functionality prediction of multi-gear pumps, Designs, vol. 8, no. 6, 2024, pp. 1-16.
[21] Ferrari, C., Morselli, S., Miccoli, G., Hamiche, K., Integrated CFD-FEM approach for external gear pump vibroacoustic field prediction, Frontiers in Mechanical Engineering, vol. 10, 2024, pp. 1-15.
[22] Hieronymus, T., Lobsinger, T., Brenner, G., A combined CFD-FEM approach to predict fluid-borne vibrations and noise radiation of a rotary vane pump, Energies, vol. 14, 2021, pp. 1-23.